Human Molecular Genetics, 2017, Vol. 26, No. 13 2377–2385

doi: 10.1093/hmg/ddx124
Advance Access Publication Date: 31 March 2017
Original Article

ORIGINAL ARTICLE

Motor neuronal repletion of the NMJ organizer, Agrin, modulates the severity of the spinal muscular atrophy disease phenotype in model mice

Jeong-Ki Kim[1,2], Charlotte Caine[1,2], Tomoyuki Awano[1,2], Ruth Herbst[3,4] and Umrao R. Monani[1,2,5,*]

[1]Department of Pathology and Cell Biology, [2]Center for Motor Neuron Biology and Disease, Columbia University Medical Center, New York, NY 10032, USA, [3]Center for Brain Research, [4]Institute of Immunology, Medical University of Vienna, 1090 Vienna and [5]Department of Neurology, Columbia University Medical Center, New York, NY 10032, USA

*To whom correspondence should be addressed at: P&S, Room 5-422, 630 W. 168th St., New York, NY 10032, USA. Tel: +212 3425132; Fax: +212 3424512; Email: um2105@columbia.edu

Abstract

Spinal muscular atrophy (SMA) is a common and often fatal neuromuscular disorder caused by low levels of the Survival Motor Neuron (SMN) protein. Amongst the earliest detectable consequences of SMN deficiency are profound defects of the neuromuscular junctions (NMJs). In model mice these synapses appear disorganized, fail to mature and are characterized by poorly arborized nerve terminals. Given one role of the SMN protein in orchestrating the assembly of spliceosomal snRNP particles and subsequently regulating the alternative splicing of pre-mRNAs, a plausible link between SMN function and the distal neuromuscular SMA phenotype is an incorrectly spliced transcript or transcripts involved in establishing or maintaining NMJ structure. In this study, we explore the effects of one such transcript—Z^+Agrin—known to be a critical organizer of the NMJ. We confirm that low SMN protein reduces motor neuronal levels of Z^+Agrin. Repletion of this isoform of Agrin in the motor neurons of SMA model mice increases muscle fiber size, enhances the post-synaptic NMJ area, reduces the abnormal accumulation of intermediate filaments in nerve terminals of the neuromuscular synapse and improves the innervation of muscles. While these effects are independent of changes in SMN levels or increases in motor neuron numbers they nevertheless have a significant effect on the overall disease phenotype, enhancing mean survival in severely affected SMA model mice by ∼40%. We conclude that Agrin is an important target of the SMN protein and that mitigating NMJ defects may be one strategy in treating human spinal muscular atrophy.

Introduction

Proximal spinal muscular atrophy (SMA) is a common, frequently fatal neuromuscular disorder caused by mutations in the Survival of Motor Neuron 1 (*SMN1*) gene and, consequently, reduced levels of its translated product, the SMN protein (1–3). In humans, an almost identical copy gene, *SMN2*, is unable to compensate for loss of *SMN1* owing to a synonymous, C→T nucleotide change in exon 7 that disrupts the splicing pattern of the homologue, rendering most of its transcripts devoid of the exon (4,5); relatively few *SMN2* transcripts remain full-length (FL). The excision of exon 7 from FL-SMN does not adversely affect the transcript, however, the resulting SMNΔ7 protein is

Received: December 15, 2016. **Revised:** February 13, 2017. **Accepted:** March 23, 2017

unstable and rapidly degraded. Accordingly, *SMN2* is reported to contribute but a fraction (10–15%) to overall levels of the functional SMN protein complex. Still, the invariable presence of *SMN2* in SMA patients ensures ubiquitous low levels of the FL-SMN protein. Moreover, the greater the number of copies of *SMN2*, the less severe is the SMA phenotype (6,7).

Rodents lack an *SMN2* gene, and breeding mice heterozygous for the single murine *Smn* gene fails to produce viable $Smn^{-/-}$ offspring (8). The embryonic lethality associated with complete loss of murine *Smn* can be rescued by expressing one or more copies of the human *SMN2* gene on the null background (9,10). What is more, *SMN2*;$Smn^{-/-}$ mice, or derivatives thereof, carrying 1–2 copies of the human transgene accurately model many aspects of the human SMA phenotype (11,12). Chief amongst these are the degeneration of the spinal motor neurons and the accompanying loss of muscle function. However, it is now clear that these signature features are preceded by an even earlier pathology of the distal motor unit. In particular, the post-synaptic specializations of mutant NMJs fail to properly mature, unable to expand in area or increase in complexity, sometimes appearing dimly stained—as if undergoing disassembly—when visualized for acetylcholine receptors (AChRs) (13–15). These post-synaptic defects are accompanied by prominent pre-synaptic abnormalities exemplified by nerve terminals swollen with neurofilament protein. The abnormal accumulation of neurofilaments in SMA terminals may be at least partly responsible for the inability to form the intricate arbors normally found at wild-type NMJs. The collective perturbations of the neuromuscular synapses, first discerned in SMA mice, were subsequently confirmed in human patients (13,16). However, it is uncertain why disrupting SMN, which is principally associated with the housekeeping functions of snRNP biogenesis and pre-mRNA splicing (17,18), would trigger such tissue-specific effects. The molecular mediators and the manner in which the NMJ defects evolve in SMA have thus, for the most part, remained elusive.

Plausible links between the canonical function of the SMN protein and NMJ phenotypes associated with a deficiency of the protein might be established through the identification of motor neuron or muscle-specific transcripts whose proper splicing is critical to the structure and/or function of the neuromuscular synapse. In this study, we explore the mediating effects of one such molecule, Agrin, which was reported mis-spliced in the motor neurons of SMA model mice (19). Agrin is expressed in motor neurons as well as muscle and best known for its role in organizing the NMJ by clustering post-synaptic acetylcholine receptors (20–22). This is accomplished chiefly through a motor neuron-derived isoform, Z^+Agrin, which is defined by the presence of an 8, 11 or 19 (8 + 11) amino acid (Z) insert that greatly enhances the ability of the molecule to cluster AChRs relative to isoforms (Z^-) devoid of it (22–24). The Z insert residues are encoded, respectively, by exons 32, 33 or both, and the incorporation of the exons into the mature transcript subject to alternative splicing. Z^+Agrin is critically important to the formation as well as maintenance of the NMJ and accomplishes this through effects on both the pre- as well as post-synaptic specializations (21,22). We demonstrate that Z^+Agrin is indeed depleted in the motor neurons of SMA model mice. Selective repletion of the protein in these cells mitigates the NMJ defects caused by SMN deficiency by enhancing post-synaptic development and reducing distal axonal pathology. This is effected without any rise in SMN levels, arrest of spinal motor neuron loss or an increase in the number of sensory inputs onto these cells. Nevertheless, the improvement in NMJ morphology translates into a modest albeit significant improvement in survival. We conclude that neuronally derived Agrin is an important mediator of the SMA phenotype and that improving NMJ function may be one means of altering the severity of the human disease.

Results

Motor neuronal repletion of Z^+Agrin modulates the phenotype of SMA model mice without altering SMN levels

Recent reports suggest that spinal motor neurons of severely affected SMA model mice express reduced levels of the Agrin isoform harboring the Z insert (Z^+Agrin) (19). We initially sought to verify this result. Quantitative PCR analysis of the anterior horn cells (motor neurons) of the spinal cords of postnatal day 3 (PND3) wild-type and SMNΔ7 SMA mice, a commonly employed model of the severe form of the human disease (25) confirmed the earlier finding. Whereas Agrin transcripts containing the Z insert were present at significantly lower levels in SMA motor neurons than in control motor neurons, transcripts lacking the insert (Z^-Agrin) were correspondingly increased in expression (Supplementary Material, Fig. S1). Accordingly, we decided to test the effects of restoring levels of Z^+Agrin to the motor neurons of SMA mice. To do so, mice expressing a chicken Z^+Agrin cDNA driven by the motor neuron-specific Hb9 promoter (26) were bred with SMA carriers, and mutants with (*Hb9:*Z^+*Agrin*;*SMN2*;*SMNΔ7*;$Smn^{-/-}$) or without (*SMN2*;*SMNΔ7*;$Smn^{-/-}$) the *Hb9:*Z^+*Agrin* transgene were generated.

Forced expression of Agrin, through inappropriate binding and activation, respectively, of the muscle-derived Lrp4 and MuSK receptors, might cause post-synaptic perturbations of the AChRs; over-expressing MuSK has been documented to trigger such effects (27). To ensure that this was not the case in the Hb9:Z^+Agrin mice, and prior to assessing the effect of restoring Z^+Agrin to SMA motor neurons, we carried out the following additional experiments. First, we examined the area of AChR clusters in muscle of 1-month-old Hb9:Z^+Agrin mice and controls. Second, we examined the width of the endplate band in the diaphragms of PND0 Hb9:Z^+Agrin transgenic animals and controls. We found that the expression of the Hb9:Z^+Agrin transgene neither altered the morphology or area of the AChRs in the adult muscle nor perturbed nerve terminals or AChR clusters in the endplate bands of newborn mice (Supplementary Material, Fig. S2A–D). We also asked if the expression of the transgene declines as is sometimes the case when the regulatory elements of the Hb9 gene are used to drive motor neuronal gene expression, and investigated the possibility of ectopic chicken Z^+Agrin expression in muscle. We found that when normalized to β-actin, the expression of the chicken Z^+Agrin transgene did not change significantly between PND7 and PND21 (Supplementary Material, Fig. S2E). When normalized to a second commonly used housekeeping gene, *Gapdh*, we found a ∼25% drop in expression between PND7 and PND14, but no further decline between PND14 and PND21 (data not shown). As expected, there was no evidence of Hb9:Z^+Agrin transgene expression in muscle (Supplementary Material, Fig. S2F).

Having ensured that the *Hb9:*Z^+*Agrin* transgene does not cause intrinsic perturbations of the NMJs, we examined the effects of restoring Z^+Agrin to the motor neurons of SMA model mice. Hereafter, SMA mice with the transgene are referred to as Z^+Agrin-SMA mutants. Although SMA model mice expressing the *Hb9:*Z^+*Agrin* transgene did not look overtly different from littermates without the transgene (Fig. 1A and B), we found that

restoring Z+Agrin to mutants did mitigate disease severity by significantly delaying death caused by very low levels of the SMN protein. Thus, whereas SMA mutants quickly succumbed to disease with a mean survival of ~9 days, littermates restored for Z+Agrin lived ~40% longer (Fig. 1C). We further showed that the chicken Z+Agrin transgene was indeed expressed in the spinal cords of Z+Agrin-SMA mutants (Fig. 1D) and was expressed at ~80% of levels of endogenous murine Z+Agrin (Fig. 1E). Total Z+Agrin in these mice is expected to equal, if not exceed by 1.3–1.5-fold, wild-type levels of the transcript. Similar results for total Z+Agrin in the Z+Agrin-SMA mutants were obtained when transcript levels were normalized to a different housekeeping gene, *Gapdh* (data not shown). To determine if Z+Agrin repletion had affected SMN levels, we examined protein concentrations in the spinal cords of the Z+Agrin-SMA mutants and control littermates. We found that SMN levels continued to be significantly lower in the spinal cords of these animals relative those in wild-type mice and no different from those in mutants without the *Hb9:Z+Agrin* transgene (Fig. 1F and G), suggesting that the mitigating effects of Z+Agrin repletion do not involve increases in SMN.

Motor neuronal repletion of Z+Agrin mitigates NMJ defects in SMA model mice

SMN deficiency triggers profound defects of the NMJs (13–15). Loss of Z+Agrin is also known to perturb the neuromuscular synapses, reducing the size and density of the post-synaptic AChRs and disrupting nerve terminal organization (22,28). To determine if motor neuronal Z+Agrin repletion had reduced the severity of the NMJ defects caused by SMN deficiency, we examined in the endplates of SMA and Z+Agrin-SMA mutants by dual staining teased gastrocnemius and triceps muscle preparations with labeled α-bungarotoxin and an antibody against neurofilament protein. While the NMJs of Z+Agrin-SMA mutants continued to display significant morphological defects relative to those of wild-type littermates, we made the following important observations suggestive of a mitigation of the abnormalities seen in mutants without the transgene (Fig. 2A). First, we found a significant improvement in nerve terminal structure. Repletion of Z+Agrin reduced the swellings of neurofilament protein characteristically seen in the terminals of SMA mice and consequently enhanced terminal arborization at the endplates (Fig. 2B). Next, we found that there were fewer denervated endplates in proximal muscles of Z+Agrin-SMA mutants compared to mutants without the *Hb9:Z+Agrin* transgene—as assessed by AChR clusters completely devoid of overlapping neurofilament staining (Fig. 2C). Conversely, Z+Agrin-SMA mutants had greater numbers of innervated endplates than did mutants without the *Hb9:Z+Agrin* transgene (Fig. 2D). Perhaps not surprisingly, the less vulnerable and distal gastrocnemius muscle showed no differences in innervation between the three cohorts of mice (Fig. 2E). Finally, we noted that the average area occupied by the post-synaptic specialization, as assessed by AChR clusters, was significantly enhanced in the triceps of Z+Agrin-SMA mice relative to that of mutants without the transgene (Fig. 3A and B). Consistent with a mitigating effect of Z+Agrin on the post-synaptic specialization, we found that the complexity of the AChR clusters was somewhat enhanced in

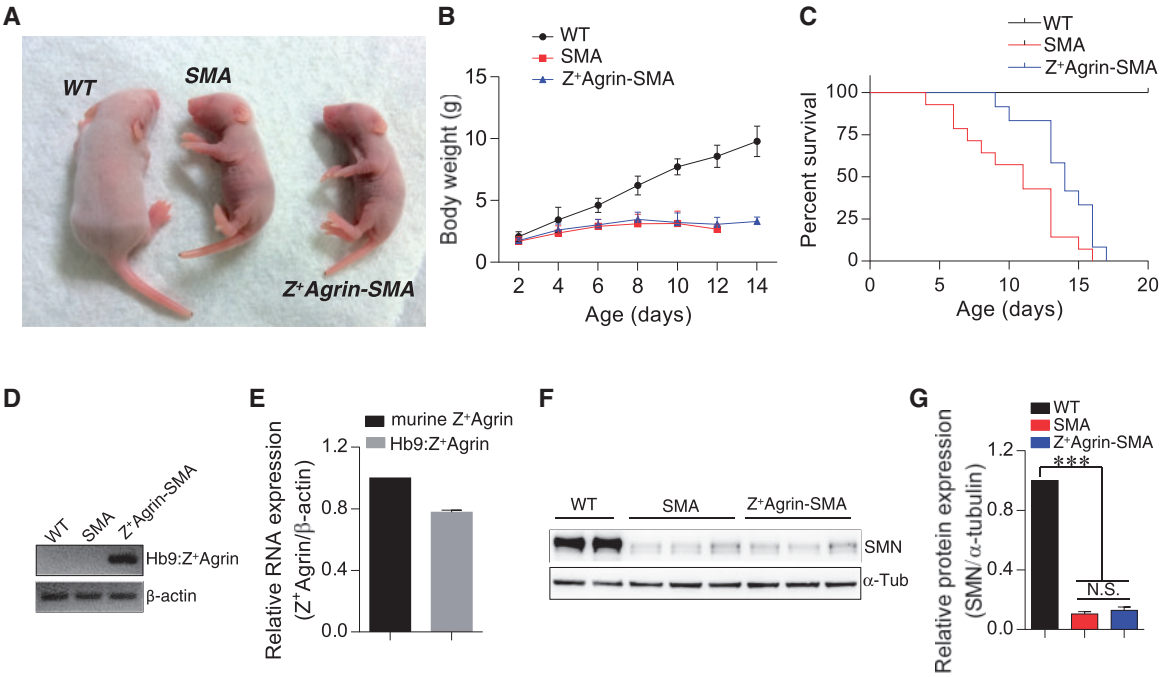

Figure 1. Augmenting Z+Agrin in motor neurons modulates the disease phenotype in SMA model mice. (**A**) Overt phenotype of a representative Z+Agrin-SMA mutant and control littermates at PND6 of life. (**B**) Weight curves of the three cohorts of mice fail to reveal significant differences between mutants with or without the *Hb9:Z+Agrin* transgene. Sample sizes = 3–11 for the individual time points. (**C**) Kaplan–Meier plots of the three cohorts of mice demonstrating a significant increase in median survival in Z+Agrin-SMA mutants relative to mutants without the transgene. $P < 0.01$, log-rank test, $n \geq 12$ for each group of mice. (**D**) Evidence of transgene RNA expression in spinal cord tissue of Z+Agrin-SMA mutants but not wild-type mice or mutants lacking the transgene. (**E**) Quantified results of transgene levels in the spinal cords of three individual Z+Agrin-SMA mutants. (**F**) Western blots of SMN protein in spinal cord tissue of Z+Agrin-SMA mutants, wild-type controls and SMA model mice that do not harbor the *Hb9:Z+Agrin* transgene. (**G**) Quantified results of western blots fail to reveal an effect of Z+Agrin augmentation on SMN levels. ***, $P < 0.001$, one-way ANOVA, $n \geq 3$ for each cohort of mice.

the Z^+Agrin-SMA mutants compared to mutants without the *Hb9:Z^+Agrin* transgene, although the difference did not reach statistical significance (Fig. 3C and D; Supplemental Material, Fig. S3). Still, the results indicate that repletion of the Z^+Agrin isoform in the motor neurons of SMA model mice mitigates both pre- as well as post-synaptic abnormalities seen in the skeletal muscles of the mutants.

Motor neuronal repletion of Z^+Agrin does not alter neurodegeneration in SMA model mice

Considering the salutary consequences of restoring Z^+Agrin on the distal motor unit of SMA model mice, we next sought to determine if similar effects could also be discerned centrally on the motor neuron cell body and furthermore on the morphology of the muscle. Accordingly, we began by quantifying the number of Choline acetyltransferase (ChAT) positive cells in the anterior horns of the spinal cords of Z^+Agrin-SMA mice and their two sets of controls. As expected, at PND11, lumbar spinal cord (L1–L3) from SMA mice without the *Hb9:Z^+Agrin* transgene had approximately half as many motor neurons as did the corresponding regions of the spinal cords of wild-type mice (Fig. 4A and B). However, we found no increase in the numbers of these cells in mutants expressing the *Hb9:Z^+Agrin* transgene (Fig. 4B). Deficiency of SMN not only results in loss of peripheral synapses but also reduces the number of central synaptic inputs to motor neurons (15,29,30). We therefore also examined motor neuron central connectivity by assessing vGlut1-positive Ia sensory inputs to the motor neurons. As in previous studies, we were able to demonstrate significantly fewer vGlut1-positive boutons on the surfaces of SMA motor neurons relative to those quantified in wild-type mice. However, akin to the negligible effect on motor neuron survival, motor neuronal Z^+Agrin repletion failed to improve the central connectivity of these cells (Fig. 4C and D). Together, these findings suggest that restoring Z^+Agrin to the motor neurons of severely affected SMA model mice neither prevents their degeneration nor mitigates the loss of central synaptic inputs to these cells.

In a final set of analyses, we examined the morphology of representative proximal and distal muscles in the two groups of SMA mice and wild-type littermates. In prior studies, we and others have reported the uniform atrophy of muscle in the

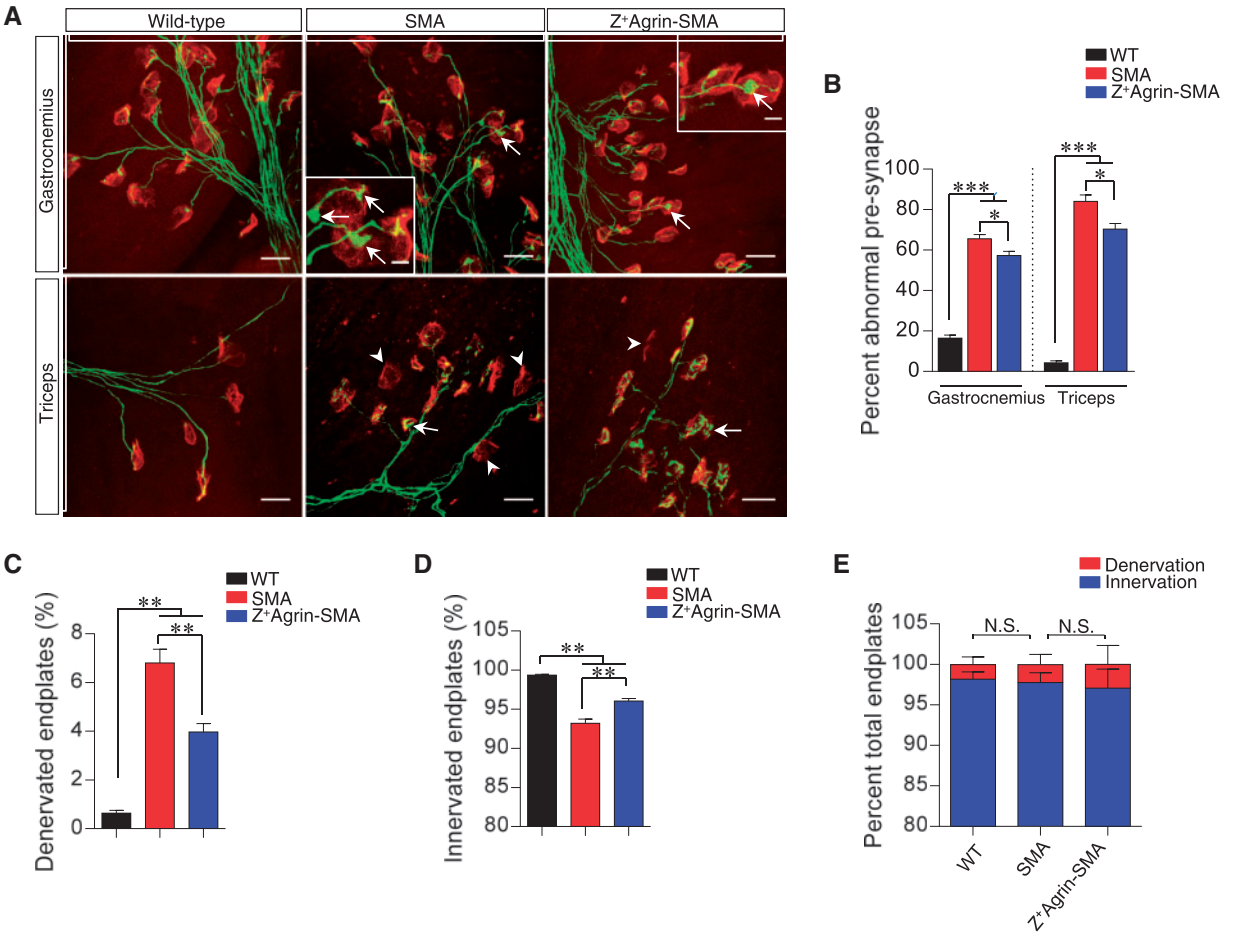

Figure 2. Restoring Z^+Agrin to the motor neurons mitigates pre-synaptic abnormalities in SMA model mice. (**A**) Immunohistochemistry of the NMJs in proximal triceps (PND11) and distal gastrocnemius (PND10) muscles of Z^+Agrin-SMA mutants depict continued albeit reduced abnormalities of the neuromuscular synapses compared to those in affected mice lacking the transgene (arrows—axon swellings; arrowheads—denervated endplates). (**B**) Graphical representation of pre-synaptic abnormalities quantified in the Z^+Agrin-SMA mutants and controls depict reduced defects following motor neuronal Z^+Agrin expression. Expression of the transgene also results in (**C**) fewer denervated endplates and (**D**) greater numbers of innervated synapses in the more proximal, vulnerable triceps. (**E**) In contrast, no differences were observed in the more distal, resistant gastrocnemius regardless of genotype. Note: *, **, ***, $P < 0.05$, < 0.01 and < 0.001, respectively, one-way ANOVA, $n \geq 100$ NMJs from each of $N \geq 3$ mice of each cohort. Scale bar: 20 μm; inset: 5 μm.

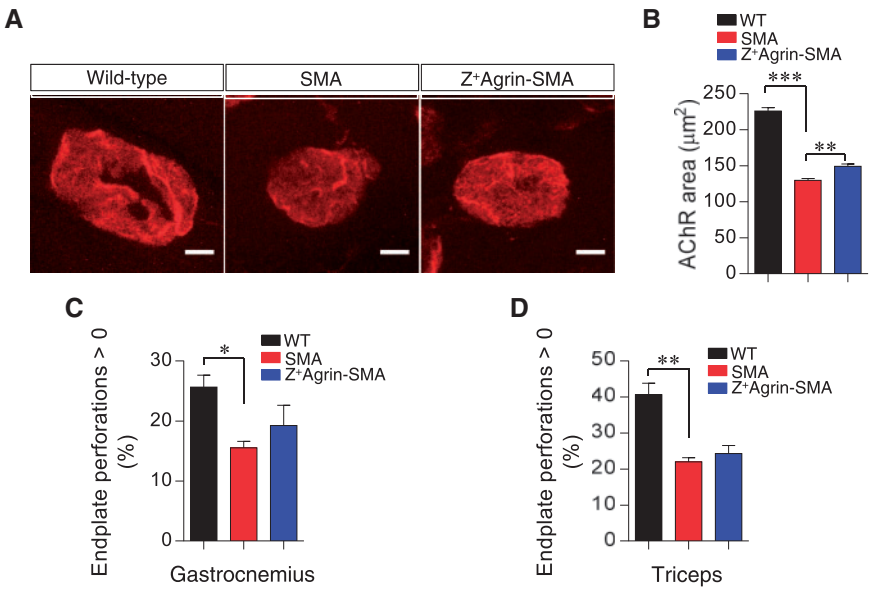

Figure 3. Restoring Z^+Agrin to the motor neurons mitigates post-synaptic abnormalities in SMA model mice. (**A**) Representative motor endplates from a PND11 wild-type mouse or SMA mutants with or without the *Hb9:Z*$^+$*Agrin* transgene, stained for AChRs with labeled α-bungarotoxin, showing a larger post-synaptic area in mutants restored for motor neuronal Z^+Agrin. Scale bar: 5 μm. (**B**) Quantification of the areas of the AChR clusters from the three cohorts of mice demonstrates a significant increase in motor endplate size in mutant mice with versus without the *Hb9:Z*$^+$*Agrin* transgene. Note: **, ***, $P < 0.01$ and < 0.001, respectively, one-way ANOVA, $n \geq 100$ NMJs from each of $N \geq 3$ mice of each cohort. An analysis of the complexity of the AChR clusters (**C, D**) based on the number of perforations noted reveals a tendency for endplates from Z^+Agrin-SMA mutants to be more elaborate than those from mutants without the transgene. Also note: *, $P < 0.05$, *t* test $n \geq 100$ NMJs from each of $N \geq 3$ mice of each cohort.

SMNΔ7 SMA model mice (9,25). Consistent with these findings, SMA muscle fibers examined in transverse sections were markedly smaller than those of wild-type, control littermates. This remained the case even in SMA mice expressing the *Hb9:Z*$^+$*Agrin* transgene (Fig. 4E–I). However, in accordance with our observations of an enhanced post-synaptic area in the Z^+Agrin SMA mice, a frequency distribution of fiber areas ordered by size from smallest to largest did reveal a perceptible shift toward the latter, relative to fibers in mutants without the transgene (Fig. 4E–G). This trend was seen in proximal as well as distal muscles. When we analyzed the data by examining mean fiber area in the three cohorts of mice, we found that Z^+Agrin-SMA mutants did indeed have significantly larger fibers than mutants lacking the transgene (Fig. 4H and I). In the proximal triceps muscles, Z^+Agrin restoration in the motor neurons resulted in a ∼30% increase in mean fiber size; in the more distal gastrocnemius, the increase was a more modest but nevertheless significant 21%. In conjunction with our analysis of the NMJs, these results suggest that restoring Z^+Agrin to the motor neurons is of greatest consequence on the distal motor unit and the muscle.

Discussion

In the years since mutations in the *SMN1* gene were found to cause SMA, much effort has been expended and rapid progress made in developing treatments for the disorder (31). The pace of the progress is owed primarily to the monogenic nature of SMA, the fortuitous existence, in humans, of the *SMN2* copy gene, the invariable presence of the gene in affected individuals and the early discovery that its expression could be modulated in a relatively straightforward manner in order to augment functional SMN levels (32,33). Accordingly, the most promising current therapeutic strategies are almost exclusively based on SMN repletion (34). While these advances, best exemplified by the recent approval of the SMN-inducing drug, Spinraza, raise much optimism for the effective treatment of pre/early-symptomatic SMA, it is clear that much remains to be uncovered about basic SMN biology. What, for instance, is the disease-relevant function of the SMN protein? Can the canonical function of SMN as a putative master regulator of RNA biogenesis explain the SMA phenotype in its entirety? If so, what are the precise mediators that link low SMN to neuromuscular dysfunction? Might identifying such mediators facilitate the development of therapeutic strategies for the symptomatic individual? The current study is an attempt to address such deficiencies in our understanding of basic SMA/SMN biology.

Three principal findings emerge from our work. First, we show that the NMJ organizer, Agrin, is indeed mis-spliced in SMA motor neurons such that abnormally low levels of the Z^+Agrin isoform are expressed in these cells. The reduction of the Z^+Agrin transcript is witnessed by an attendant increase in the transcript (Z^-Agrin) lacking the Z insert. Second, we demonstrate that motor neuronal repletion of the Z^+Agrin isoform is sufficient to have a modest but notable mitigating effect on the severe SMA phenotype of SMNΔ7 model mice. Enhanced survival of the Z^+Agrin-SMA mutants is accompanied by enlarged muscle fibers and improved morphology of the distal motor unit. Central synaptic defects, on the other hand, remain in Z^+Agrin-SMA mutants. Finally, our experimental results show that Agrin is likely only one of several key targets of the SMN complex. Motor neuron loss is not arrested and Z^+Agrin-SMA mutants continue to exhibit an accelerated rate of mortality resulting from low SMN protein.

Agrin is one of the principal organizers of the mammalian NMJ. This function is mediated primarily by its alternatively

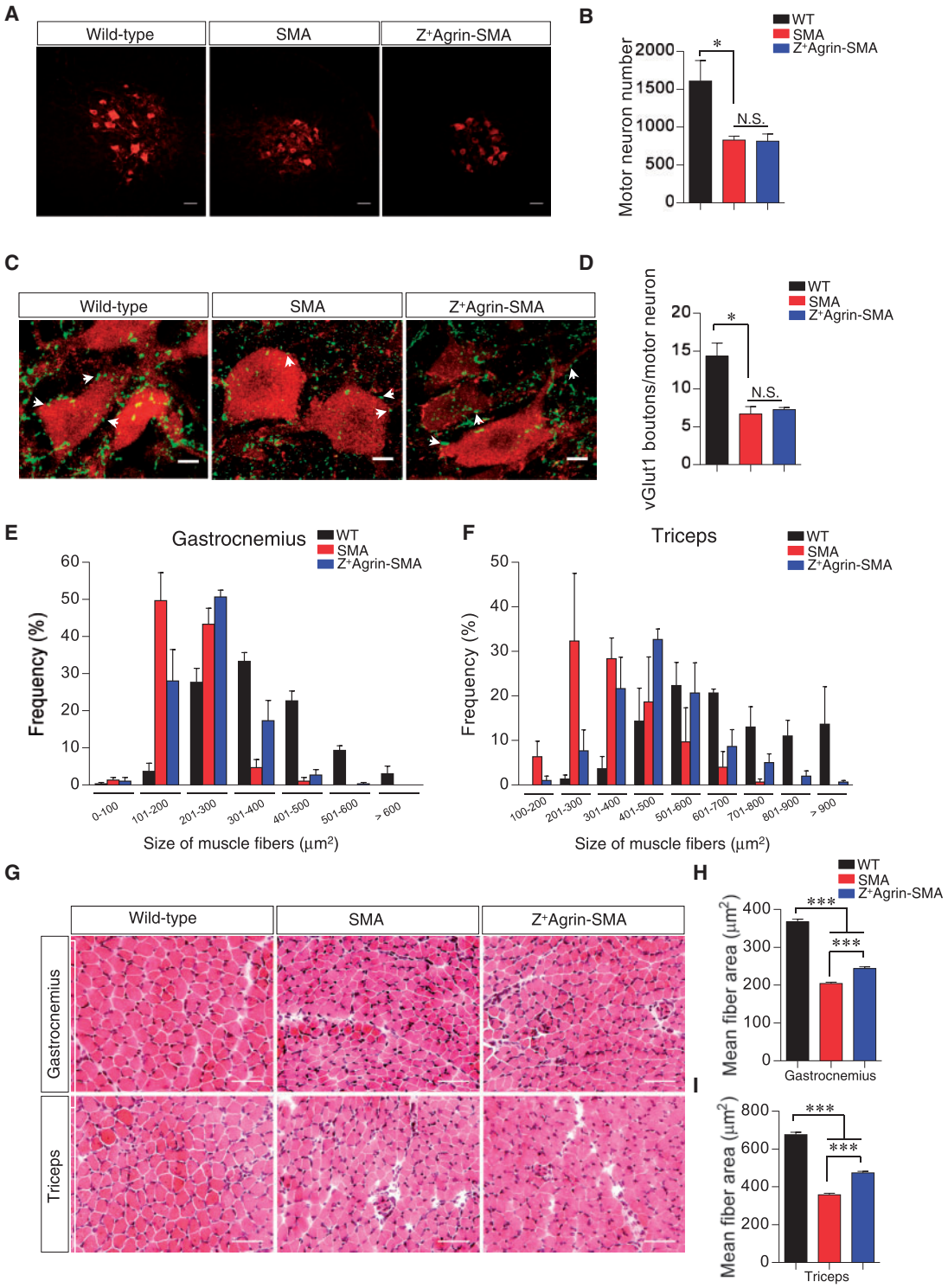

Figure 4. Muscle size but not motor neuron pathology is improved in SMA mice augmented for Z^+Agrin. (**A**) Immunohistochemistry for ChAT-positive motor neurons in spinal cord tissue of PND11 Z^+Agrin-SMA mutants and controls shows that restoring Z^+Agrin fails to arrest neurodegeneration and does not result in greater numbers of these cells. Scale bar: 50 μm. (**B**) Graph depicting quantification of the motor neurons in the three cohorts of mice. (**C**) Spinal motor neurons from PND11 Z^+Agrin-SMA mutants and controls dual labeled with ChAT and vGlut1 to assess central synaptic connectivity in response to restoring Z^+Agrin to these cells. Arrows depict vGlut1 boutons. Scale bar: 10 μm. (**D**) A quantification of vGlut1 boutons on the motor neurons of the three cohorts of mice demonstrates that restoring Z^+Agrin does little to improve central synaptic inputs to these cells. Frequency distributions of muscle fibers in the (**E**) gastrocnemius and (**F**) triceps of PND10 mice are indicative of an increase in fiber size following expression of the *Hb9:Z⁺Agrin* transgene in SMA mutants. (**G**) Representative muscle sections from the gastrocnemius and triceps of the three cohorts of mice stained with hematoxylin and eosin at PND10. Scale bar: 50 μm. A quantification of the areas of the fibers in the (**H**) distal gastrocnemius and (**I**) proximal triceps demonstrates a significant increase in muscle fiber size upon augmenting Z^+Agrin in SMA mutants. Note: *, **, ***, $P < 0.05$, < 0.01 and < 0.001, respectively, one-way ANOVA, $N \geq 3$ mice of each genotype and $n \geq 100$ muscle fibers from each individual mouse where applicable.

spliced Z^+ isoform, a molecule defined by an 8, 11 or 19 amino acid "Z" insert derived, respectively, from exons 32, 33 or both of the corresponding gene. Expressed by motor neurons and secreted into the basal lamina of the neuromuscular synapse, Z^+Agrin is a potent clustering factor of the post-synaptic AChRs and acts to counter the dispersing activity of the neurotransmitter, acetylcholine (35). This is accomplished through the activation of a post-synaptic receptor complex consisting of the Lrp4 protein and the receptor tyrosine kinase, MuSK (36–38). In the absence of Z^+Agrin, the NMJs are profoundly disrupted and animals die during the perinatal period. At the post-synaptic specialization, AChR clusters are reduced in number, size and density and frequently devoid of an innervating nerve, while at the presynaptic end, terminal differentiation is perturbed with exuberant outgrowth of axons in embryos, and atrophy, swellings or poor arborization in adults (21,22,28). Interestingly, these characteristic NMJ abnormalities phenocopy some aspects of the neuromuscular synaptic defects that we and others have reported observing in SMA model mice (15,39,40). Co-incidentally, it has recently emerged that SMA motor neurons express reduced levels of the Z^+Agrin isoform (19) suggesting that at least some of the NMJ defects in SMA might be attributed to disrupted Agrin signaling. Other RNA-profiling studies similar to those of Zhang *et al*, which prompted us to examine the effects of Z^+Agrin repletion in SMA, did not report perturbations in this transcript (41–43). However, this lack of congruence may not be entirely surprising; the studies varied considerably with respect to the source tissue analyzed—primary motor neurons, whole spinal cord, laser-capture microdissected motor neurons and ES cell-derived motor neurons—and the precise type of analysis conducted—microarrays versus RNA-Seq.

Our results have confirmed perturbations of Z^+Agrin in the motor neurons of a severely affected SMA mouse model. The modest but significant improvement in NMJ morphology along with an overall delay in mortality supports the contention that Agrin is a genuine target of the SMN protein and a *bona fide* link between the canonical splicing function of SMN and a predominantly neuromuscular SMA phenotype. That Z^+Agrin repletion fails to more fully ameliorate the disease phenotype might merely signal that it is but one of several SMN targets whose functions must be restored in the very severe SMNΔ7 mouse model of SMA. Whether perturbations in the other determinants of the SMA phenotype are a consequence of disruptions in SMN-mediated splicing or some hitherto undefined function remains to be determined. One set of appealing candidates—also established, muscle-derived synaptic organizers—that are nevertheless susceptible to disruptions in SMN-mediated splicing and would thus constitute additional links between the canonical function of the protein and neuromuscular dysfunction are the laminins. Validating these will require a careful analysis akin to the one we describe here for Agrin. A more unbiased approach could exploit observations of the temporal requirements for the SMN protein, in particular the abrupt transition from an SMN-sensitive to an SMN-resistant state that happens to coincide with the appearance of the fully mature NMJ (44). The rapidity of the transition could imply that there is a factor whose function is dependent on wild-type SMN levels and whose activity is required for final NMJ maturation. Identifying such factors, indeed the constellation of critical SMN mediators, is almost certain to shed light on how low protein triggers a primary neuromuscular disease phenotype. One or more of the mediators may also turn out to be novel targets for the treatment of SMA during late (post-symptomatic) stages of the disease.

Materials and Methods

Mice

SMNΔ7 SMA model mice (Jax #005025) were maintained on a predominantly FVB/N genetic strain background and genotyped as previously described (25). Transgenic mice carrying the chicken Z^+Agrin cDNA driven by the regulatory elements of the Hb9 gene (26) were a gift from Dr. S. Burden and initially recovered in the C57Bl/6 strain from frozen sperm as previously described (45). Such mice were bred to SMA carriers and the resulting progeny backcrossed to the carriers to generate *Hb9:Z$^+$Agrin*-positive animals homozygous for the *SMN2* and *SMNΔ7* transgenes. SMA mutants with or without one copy of the *Hb9:Z$^+$Agrin* transgene were produced by crossing SMA carriers (*SMN2;SMNΔ7;Smn$^{+/-}$*) with carriers harboring the transgene (*Hb9:Z$^+$Agrin;SMN2;SMNΔ7;Smn$^{+/-}$*). The *Hb9:Z$^+$Agrin* transgene was detected by PCR as previously described (ref. 26 and also see Supplementary Material, Table S1 for list of primers used to genotype the mice). Body weights and survival data were compiled as described by us in a previous study (13). All animal procedures were performed according to institutional guidelines.

Laser capture microdissection

Lumbar spinal cord was dissected from PND3 mice, embedded in Tissue-Tek OCT medium (Fisher Scientific) and frozen in dry ice. Spinal cord transverse sections (12 μm) were cut on a cryostat (Leica 3050S), transferred to PEN membrane slides (Zeiss, Germany) and stained with Cresyl Violet using an LCM staining kit (Thermofisher Scientific). Approximately 1200 cell bodies from 55 to 60 spinal cord sections (per mouse) were microdissected on a Leica DM6000b microscope equipped with a 20× objective and RNA extracted and purified using an RNeasy Plus Micro Kit (Qiagen, CA).

Motor neuron counts and muscle analysis

For motor neuron counts and vGlut1 input analysis, spinal cord tissue was dissected following transcardial perfusion (4% PFA in 1× PBS) of mice. The tissue was post-fixed in the same fixative, cryo-protected in first 20% and then 30% sucrose before embedding the material in Tissue-Tek OCT medium for cryostat sections. 20 μm sections from L1 to L3 spinal cords were overlaid for 10 min with 4% PFA, washed in 1× TBS and the tissue then permeabilized with 0.5% Triton X-100 (5 min). To stain the motor neurons, sections were placed in blocking buffer (2% normal serum, 3% BSA, 0.1% Triton X-100 in TBST) for 1 h. The sections were then incubated (4°C, overnight) with primary antibodies against ChAT (1:100, Millipore) and vGlut1 (1:10 000, Millipore) diluted in blocking buffer, following which they were washed (4 × 15 min) in 1× TBST. They were then incubated with secondary antibodies (Alexa Fluor-594 conjugated donkey anti-goat IgG or Alexa Fluor-488 conjugated goat anti-guinea pig IgG) each at dilutions of 1:1000. After a second round of washing (4 × 15 min) in 1× TBST, the sections were mounted in anti-fade mounting media (Vector Labs) and motor neurons visualized either or a Nikon 80i fluorescent microscope (Nikon) or a Leica TCS SP5 II laser scanning confocal microscope (Leica). For muscle analysis, the proximal triceps or distal gastrocnemius were flash-frozen in isopentane cooled with liquid nitrogen. 12 μm thick sections were stained with hematoxylin and eosin (Sigma) and fiber morphology assessed as previously described

(46). Quantification of the neuropathology was performed in a blinded manner.

Analysis of NMJs

NMJ analysis was performed on whole muscle, fixed and permeabilized with 100% methanol for 10 min at −20°C, and incubated with blocking buffer as described above for 1 h. The tissue was sequentially incubated for overnight periods at 4°C with an anti-neurofilament antibody (1:1000, Millipore), Alexa Fluor-488 conjugated donkey anti-rabbit IgG secondary antibody (1:1000, Invitrogen) and rhodamine-α-bungarotoxin (1:1000, Invitrogen). Each incubation was followed by a washing step (4 × 15 min; 1× TBST). The tissue was mounted in anti-fade medium (Vector Labs) and images of NMJs acquired by confocal microscopy as described above. A quantification of innervated NMJs, defective terminals and motor endplates was performed as previously described (13,15,29). The various NMJ parameters were compiled by investigators unaware of the genotypes of the mice.

Western blotting and quantitative RT-PCR

SMN protein levels in PND10 animals were analyzed by western blotting using standard procedures described previously (9). Monoclonal antibodies to SMN (1:5000, BD Biosciences) and β-tubulin (1:10 000, Sigma) were used to probe the blot and the resulting bands visualized using the ECL kit (GE Healthcare). The thoracic segment of the spinal cord was used for extracting total RNA using TRIZOL (Invitorgen) according to the manufacturer's instructions. Following cDNA synthesis, quantitative RT-PCR was performed in triplicate on a MasterCycler Real Plex4 (Eppendorf). Sequences of gene specific primers for the RT-PCR are detailed in Supplementary Material, Table S1.

Statistics

Kaplan-Meier survival curves were compared and assessed for differences using the log-rank test equivalent to the Mantel-Haenszel test. The unpaired, 2-tailed Student's *t* test or 1-way ANOVA followed by Tukey's post-hoc comparison, where indicated, were used to compare means for statistical differences. Data are represented as mean ± SEM unless otherwise indicated. $P < 0.05$ was considered significant. Statistical analyses were performed with GraphPad Prism v6.0 (GraphPad Software).

Supplementary Material

Supplementary Material is available at *HMG* online.

Acknowledgements

We thank members of the Monani lab for insightful discussions and comments on the manuscript. We would further like to express our sincere gratitude to Dr. S. J. Burden for sharing the Hb9:Z^{+}Agrin mice with us and to Monica Mendelsohn for assisting with their recovery.

Conflict of Interest statement. None declared.

Funding

This work was supported by grants from the Muscular Dystrophy Association of America, AFM-France, and National Institutes of Health (NS057482 to U.R.M.). Work in the Herbst lab is funded through the Austrian Science Fund (P28485-B27).

References

1. Lefebvre, S., Burglen, L., Reboullet, S., Clermont, O., Burlet, P., Viollet, L., Benichou, B., Cruaud, C., Millasseau, P., Zeviani, M. *et al*. (1995) Identification and characterization of a spinal muscular atrophy-determining gene. *Cell*, **80**, 155–165.
2. Lefebvre, S., Burlet, P., Liu, Q., Bertrandy, S., Clermont, O., Munnich, A., Dreyfuss, G. and Melki, J. (1997) Correlation between severity and SMN protein level in spinal muscular atrophy. *Nat. Genet.*, **16**, 265–269.
3. Coovert, D.D., Le, T.T., McAndrew, P.E., Strasswimmer, J., Crawford, T.O., Mendell, J.R., Coulson, S.E., Androphy, E.J., Prior, T.W. and Burghes, A.H. (1997) The survival motor neuron protein in spinal muscular atrophy. *Hum. Mol. Genet.*, **6**, 1205–1214.
4. Monani, U.R., Lorson, C.L., Parsons, D.W., Prior, T.W., Androphy, E.J., Burghes, A.H. and McPherson, J.D. (1999) A single nucleotide difference that alters splicing patterns distinguishes the SMA gene SMN1 from the copy gene SMN2. *Hum. Mol. Genet.*, **8**, 1177–1183.
5. Lorson, C.L. and Androphy, E.J. (2000) An exonic enhancer is required for inclusion of an essential exon in the SMA-determining gene SMN. *Hum. Mol. Genet.*, **9**, 259–265.
6. McAndrew, P.E., Parsons, D.W., Simard, L.R., Rochette, C., Ray, P.N., Mendell, J.R., Prior, T.W. and Burghes, A.H. (1997) Identification of proximal spinal muscular atrophy carriers and patients by analysis of SMNT and SMNC gene copy number. *Am. J. Hum. Genet.*, **60**, 1411–1422.
7. Feldkotter, M., Schwarzer, V., Wirth, R., Wienker, T.F. and Wirth, B. (2002) Quantitative analyses of SMN1 and SMN2 based on real-time lightCycler PCR: fast and highly reliable carrier testing and prediction of severity of spinal muscular atrophy. *Am. J. Hum. Genet.*, **70**, 358–368.
8. Schrank, B., Gotz, R., Gunnersen, J.M., Ure, J.M., Toyka, K.V., Smith, A.G. and Sendtner, M. (1997) *Proc. Natl. Acad. Sci. USA.*, **94**, 9920–9925.
9. Monani, U.R., Sendtner, M., Coovert, D.D., Parsons, D.W., Andreassi, C., Le, T.T., Jablonka, S., Schrank, B., Rossol, W., Prior, T.W. *et al*. (2000) The human centromeric survival motor neuron gene (SMN2) rescues embryonic lethality in smn(−/−) mice and results in a mouse with spinal muscular atrophy. *Hum. Mol. Genet.*, **9**, 333–339.
10. Hsieh-Li, H.M., Chang, J.G., Jong, Y.J., Wu, M.H., Wang, N.M., Tsai, C.H. and Li, H. (2000) A mouse model for spinal muscular atrophy. *Nat. Genet.*, **24**, 66–70.
11. Sleigh, J.N., Gillingwater, T.H. and Talbot, K. (2011) The contribution of mouse models to understanding the pathogenesis of spinal muscular atrophy. *Dis. Model Mech.*, **4**, 457–467.
12. Park, G.H., Kariya, S. and Monani, U.R. (2010) Spinal muscular atrophy: new and emerging insights from model mice. *Curr. Neurol. Neurosci. Rep.*, **10**, 108–117.
13. Kariya, S., Park, G.H., Maeno-Hikichi, Y., Leykekhman, O., Lutz, C., Arkovitz, M.S., Landmesser, L.T. and Monani, U.R. (2008) Reduced SMN protein impairs maturation of the neuromuscular junctions in mouse models of spinal muscular atrophy. *Hum. Mol. Genet.*, **17**, 2552–2569.
14. Murray, L.M., Comely, L.H., Thomson, D., Parkinson, N., Talbot, K. and Gillingwater, T.H. (2008) Selective vulnerability of motor neurons and dissociation of pre- and post-synaptic pathology at the neuromuscular junction in mouse models of spinal muscular atrophy. *Hum. Mol. Genet.*, **17**, 949–962.

15. Ling, K.K., Lin, M.Y., Zingg, B., Feng, Z. and Ko, C.-P. (2010) Synaptic defects in the spinal and neuromuscular circuitry in a mouse model of spinal muscular atrophy. *PLoS One*, **5**, e15457.
16. Martínez-Hernández, R., Bernal, S., Also-Rallo, E., Alías, L., Barceló, M.J., Hereu, M., Esquerda, J.E. and Tizzano, E.F. (2013) Synaptic defects in type I spinal muscular atrophy in human development. *J. Pathol.*, **229**, 49–61.
17. Kolb, S.J., Battle, D.J. and Dreyfuss, G. (2007) Molecular functions of the SMN complex. *J. Child Neurol.*, **22**, 990–994.
18. Tisdale, S. and Pellizzoni, L. (2015) Disease mechanisms and therapeutic approaches in spinal muscular atrophy. *J. Neurosci.*, **35**, 8691–8700.
19. Zhang, Z., Pinto, A.M., Wan, L., Wang, W., Berg, M.G., Oliva, I., Singh, L.N., Dengler, C., Wei, Z. and Dreyfuss, G. (2013) Dysregulation of synaptogenesis genes antecedes motor neuron pathology in spinal muscular atrophy. *Proc. Natl. Acad. Sci. USA.*, **110**, 19348–19353.
20. Misgeld, T., Kummer, T.T., Lichtman, J.W. and Sanes, J.R. (2005) Agrin promotes synaptic differentiation by counteracting an inhibitory effect of neurotransmitter. *Proc. Natl. Acad. Sci. USA.*, **102**, 11088–11093.
21. Gautam, M., Noakes, P.G., Moscoso, L., Rupp, F., Scheller, R.H., Merlie, J.P. and Sanes, J.R. (1996) Defective neuromuscular synaptogenesis in agrin-deficient mutant mice. *Cell*, **85**, 525–535.
22. Burgess, R.W., Nguyen, Q.T., Son, Y.J., Lichtman, J.W. and Sanes, J.R. (1999) Alternatively spliced isoforms of nerve- and muscle-derived agrin: their roles at the neuromuscular junction. *Neuron*, **23**, 33–44.
23. Gesemann, M., Denzer, A.J. and Ruegg, M.A. (1995) Acetylcholine receptor-aggregating activity of agrin isoforms and mapping of the active site. *J. Cell. Biol.*, **128**, 625–636.
24. Hoch, W., Campanelli, J.T., Harrison, S. and Scheller, R.H. (1994) Structural domains of agrin required for clustering of nicotinic acetylcholine receptors. *EMBO J.*, **13**, 2814–2821.
25. Le, T.T., Pham, L.T., Butchbach, M.E., Zhang, H.L., Monani, U.R., Coovert, D.D., Gavrilina, T.O., Xing, L., Bassell, G.J. and Burghes, A.H. (2005) SMNDelta7, the major product of the centromeric survival motor neuron (SMN2) gene, extends survival in mice with spinal muscular atrophy and associates with full-length SMN. *Hum. Mol. Genet.*, **14**, 845–857.
26. Ruggiu, M., Herbst, R., Kim, N., Jevsek, M., Fak, J.J., Mann, M.A., Fischbach, G., Burden, S.J. and Darnell, R.B. (2009) Rescuing Z+ agrin splicing in Nova null mice restores synapse formation and unmasks a physiologic defect in motor neuron firing. *Proc. Natl. Acad. Sci. USA.*, **106**, 3513–3518.
27. Kim, N. and Burden, S.J. (2008) MuSK controls where motor axons grow and form synapses. *Nat. Neurosci.*, **11**, 19–27.
28. Samuel, M.A., Valdez, G., Tapia, J.C., Lichtman, J.W. and Sanes, J.R. (2012) Agrin and synaptic laminin are required to maintain adult neuromuscular junctions. *PLoS One*, **7**, e46663.
29. Park, G.H., Maeno-Hikichi, Y., Awano, T., Landmesser, L.T. and Monani, U.R. (2010) Reduced survival of motor neuron (SMN) protein in motor neuronal progenitors functions cell autonomously to cause spinal muscular atrophy in model mice expressing the human centromeric (SMN2) gene. *J. Neurosci.*, **30**, 12005–12019.
30. Mentis, G.Z., Blivis, D., Liu, W., Droba, c. E., Crowder, M.E., Kong, L., Alvarez, F.J., Sumner, C.J. and O'Donovan, M.J. (2011) Early functional impairment of sensory-motor connectivity in a mouse model of spinal muscular atrophy. *Neuron*, **69**, 453–467.
31. Monani, U.R. and De Vivo, D.C. (2014) Neurodegeneration in spinal muscular atrophy: from disease phenotype and animal models to therapeutic strategies and beyond. *Future Neurol.*, **9**, 49–65.
32. Singh, N.K., Singh, N.N., Androphy, E.J. and Singh, R.N. (2006) Splicing of a critical exon of human Survival Motor Neuron is regulated by a unique silencer element located in the last intron. *Mol. Cell. Biol.*, **26**, 1333–1346.
33. Hua, Y., Vickers, T.A., Baker, B.F., Bennett, C.F. and Krainer, A.R. (2007) Enhancement of SMN2 exon 7 inclusion by antisense oligonucleotides targeting the exon. *PLoS Biol.*, **5**, e73.
34. Gillingwater, T.H. and Murray, L.M. (2015) How far away is spinal muscular atrophy gene therapy?. *Expert. Rev. Neurother.*, **9**, 965–968.
35. Kummer, T.T., Misgeld, T. and Sanes, J.R. (2006) Assembly of the postsynaptic membrane at the neuromuscular junction: paradigm lost. *Curr. Opin. Neurobiol.*, **16**, 74–82.
36. DeChiara, T.M., Bowen, D.C., Valenzuela, D.M., Simmons, M.V., Poueymirou, W.T., Thomas, S., Kinetz, E., Compton, D.L., Rojas, E., Park, J.S. *et al.* (1996) The receptor tyrosine kinase MuSK is required for neuromuscular junction formation in vivo. *Cell*, **85**, 501–512.
37. Glass, D.J., Bowen, D.C., Stitt, T.N., Radziejewski, C., Bruno, J., Ryan, T.E., Gies, D.R., Shah, S., Mattsson, K., Burden, S.J. *et al.* (1996) Agrin acts via a MuSK receptor complex. *Cell*, **85**, 513–523.
38. Kim, N., Stiegler, A.L., Cameron, T.O., Hallock, P.T., Gomez, A.M., Huang, J.H., Hubbard, S.R., Dustin, M.L. and Burden, S.J. (2008) Lrp4 is a receptor for Agrin and forms a complex with MuSK. *Cell*, **135**, 334–342.
39. Kong, L., Wang, X., Choe, D.W., Polley, M., Burnett, B.G., Bosch-Marcé, M., Griffin, J.W., Rich, M.M. and Sumner, C.J. (2009) Impaired synaptic vesicle release and immaturity of neuromuscular junctions in spinal muscular atrophy mice. *J. Neurosci.*, **29**, 842–851.
40. Kariya, S., Mauricio, R., Dai, Y. and Monani, U.R. (2009) The neuroprotective factor Wld(s) fails to mitigate distal axonal and neuromuscular junction (NMJ) defects in mouse models of spinal muscular atrophy. *Neurosci. Lett.*, **449**, 246–251.
41. Baümer, D., Lee, S., Nicholson, G., Davies, S., Parkinson, N.J., Murray, L.M., Gillingwater, T.H., Ansorge, O., Davies, K.E. and Tallbot, K. (2009) Alternative splicing events are a late feature of pathology in a mouse model of spinal muscular atrophy. *PLoS Genet.*, **12**, e1000773.
42. Maeda, M., Harris, A.W., Kingham, B.F., Lumpkin, C.J., Opdenaker, L.M., McCahan, S.M., Wang, W. and Butchbach, M.E. (2014) Transcriptome profiling of spinal muscular atrophy motor neurons derived from mouse embryonic stem cells. *PLoS One*, **9**, e106818.
43. Saal, L., Briese, M., Kneitz, S., Glinka, M. and Sendtner, M. (2014) Subcellular transcriptome alterations in a cell culture model of spinal muscular atrophy point to widespread defects in axonal growth and presynaptic differentiation. *RNA*, **20**, 1789–1802.
44. Kariya, S., Obis, T., Garone, C., Akay, T., Sera, F., Iwata, S., Homma, S. and Monani, U.R. (2014) Requirement of enhanced Survival Motoneuron protein imposed during neuromuscular junction maturation. *J. Clin. Invest.*, **124**, 785–800.
45. Li, M.W., Glass, O.C., Zarrabi, J., Baker, L.N. and Lloyd, K.C. (2016) Cryorecovery of mouse sperm by different IVF methods using MBCD and GSH. *J. Fertili. In Vitro*, **4**, pii: 175.
46. Monani, U.R., Pastore, M.T., Gavrilina, T.O., Jablonka, S., Le, T.T., Andreassi, C., DiCocco, J.M., Lorson, C., Androphy, E.J., Sendtner, M. *et al.* (2003) A transgene carrying an A2G missense mutation in the SMN gene modulates phenotypic severity in mice with severe (type I) spinal muscular atrophy. *J. Cell. Biol.*, **160**, 41–52.